

Polarimetry Using Liquid Crystal Variable Retarders

© 2005 Meadowlark Optics, Inc.

Thomas F. Drouillard II^{*a}, Paul A. Searcy^a, Scott R. Davis^b, Radoslaw J. Uberna^b, Richard A. Herke^b, Michael H. Anderson^b, Scott D. Rommel^b, Eric B. Anthony^b, Valeria B. Damiao^b

^aMeadowlark Optics, Inc. PO Box 1000, Frederick, Colorado, USA 80530;

^bFormerly of Meadowlark Optics, Inc. PO Box 1000, Frederick, Colorado, USA 80530

ABSTRACT

A new technology for performing high-precision Stokes polarimetry is presented. One traditional Stokes polarimetry configuration relies on mechanical devices such as rapidly rotating waveplates that are undesirable in vibration-sensitive optics experiments. Another traditional technique requires division of a light signal into four components that are measured individually; this technique is limited to applications in which signal levels are sufficient that intensity reduction does not diminish the signal-to-noise ratio. A new technology presented here is similar to the rotating waveplate approach, but two liquid crystal variable retarders (LCVR's) are used instead of waveplates. A Stokes polarimeter instrument based on this technology has been made commercially available. The theory of operation is detailed, and an accuracy assessment was conducted. Measurement reproducibility was verified and used to produce empirical estimates of uncertainty in measured components of a Stokes vector. Uncertainty propagation was applied to polarization parameters calculated from Stokes vector components to further the accuracy assessment. A calibrated polarimeter measures four Stokes components with 10^{-3} precision and average predicted uncertainties less than $\pm 2 \times 10^{-3}$. An experiment was conducted in which the linear polarization angles were measured with a LC polarimeter and with a photodiode for comparison. Observed discrepancies between polarization angle measurements made with a polarimeter and those made with a photodetector were nominally within $\pm 0.3^\circ$.

Keywords: Polarimeter, polarization, birefringence, retarder, waveplate, liquid crystal, Stokes, Mueller

NOMENCLATURE

Variables

- E_H Magnitude of the horizontally-directed electric field component of linearly-polarized light.
- E_V Magnitude of the vertically-directed electric field component of linearly-polarized light.
- I_H Intensity of the horizontal component of linearly-polarized light, measured with a photodetector.
- I_V Intensity of the vertical component of linearly-polarized light, measured with a photodetector.
- I_C Intensity of the (horizontal + vertical) combined components of linearly-polarized light, measured with a photodetector.
- SOP* State of Polarization
- DOP* Degree of Polarization
-

DOLP Degree of Linear Polarization

DOCP Degree of Circular Polarization

ε Ellipticity of a polarization ellipse.

□ Azimuth of the major axis of a polarization ellipse, or the orientation of a linear state of polarization.

□ Uncertainty associated with a measured or calculated value.

S A four-component time-invariant Stokes vector that describes the polarization state of light incident upon the polarimeter.

S_0 The first Stokes component (intensity)

S_1 The second Stokes component (difference between horizontal and vertical linear components)

S_2 The third Stokes component (difference between $+45^\circ$ and -45° linear components)

S_3 The fourth Stokes component (difference between right and left circular components)

$\mathbf{S}(\square)(t)$ A four-component Stokes vector that models the polarization state of light incident on the polarimeter detector after passing through the optics of the polarimeter. The time-dependence arises due to varying of the polarization by the polarimeter optics.

$S(\square)(t)$ The first component of the Stokes vector that models the time-varying light signal incident upon the polarimeter detector after passing through the optics of the polarimeter. This component is the intensity of light at the detector, therefore it is the signal that is measured by the detector.

$\mathbf{M}(t)$ The 4×4 Mueller matrix that models the time-varying optical effect of the polarimeter on an incident, time-invariant light signal.

$a_i(t)$ The first column, i^{th} row component of $\mathbf{M}(t)$; these terms act on S_0 .

$b_i(t)$ The second column, i^{th} row component of $\mathbf{M}(t)$; these terms act on S_1 .

$c_i(t)$ The third column, i^{th} row component of $\mathbf{M}(t)$; these terms act on S_2 .

$d_i(t)$ The fourth column, i^{th} row component of $\mathbf{M}(t)$; these terms act on S_3 .

Subscripts and Superscripts:

■ □ *e.g.* $\mathbf{S}'(t)$ denotes Stokes vector and vector components of light that has passed through polarimeter optics.

■ $0, 1, 2, 3$ *e.g.* $S_0(t)$ denotes the row number of a Stokes vector or Mueller matrix.

■ H, V *e.g.* \mathbf{S}_H denotes horizontal or vertical linearly polarized light.

e.g. $S'_{0,H}(t)$ denotes a detected light signal resulting from horizontal or vertical linearly polarized light passing through polarimeter optics.

■ $+45, -45$ *e.g.* \mathbf{S}_{+45} denotes $\pm 45^\circ$ linearly polarized light.

e.g. $S_{0,+45}(t)$ denotes a detected light signal resulting from $\pm 45^\circ$ linearly polarized light passing through polarimeter optics.

■ R, L *e.g.* \mathbf{S}_R denotes right or left circularly polarized light.

e.g. $S'_{0,R}(t)$ denotes a detected light signal resulting from right or left circularly polarized light passing through polarimeter optics.

1. INTRODUCTION

Polarization is the state or behavior of the transverse electric field of a light wave. Since the electric component of light is measurably affected by interaction of light with matter and energy, the polarization characteristics of light can provide diagnostic information for a broad range of applications. Remote sensing, solar astronomy, atomic and molecular spectroscopy, and

materials analysis are examples of the fields in which polarization measurements are employed. For example, solar magnetic field measurements can be obtained by polarization analysis of certain components of the solar spectrum.¹ Surface roughness and anisotropy of materials can be determined by investigating the depolarization of light upon reflection.

An overview of polarization principles appears in most general optics texts,^{2, 3} and there are books dedicated solely to the topic of polarization.^{4, 5} Here we begin with a brief discussion of polarization using Stokes vector nomenclature and basic polarization optics primarily derived from [5]. We detail a technique implemented in a commercially available liquid crystal polarimeter by which the components of a Stokes vector are detected (i.e., the complete state of polarization is determined).⁶ We present uncertainty estimates of the measured Stokes components, and propagate those uncertainties through parameters calculated from the Stokes vector. We present experimental data demonstrating polarimetric precision and uncertainty.

2. BASIC POLARIZATION THEORY

The state of polarization (*SOP*) is a mathematical construct that uses a vector convention to completely describe the time-averaged electric field components of a light wave. The Stokes formalism is a four-component vector:

$$S = \begin{bmatrix} S_0 \\ S_1 \\ S_2 \\ S_3 \end{bmatrix}$$

where:

S_0 = total light intensity (normalized, $\therefore 0 \leq S_0 \leq 1$).

S_1 = difference between horizontal and vertical intensity components ($-1 \leq S_1 \leq 1$).

S_2 = difference between intensity components oriented at $\pm 45^\circ$ ($-1 \leq S_2 \leq 1$).

S_3 = intensity difference between right and left circular intensity components ($-1 \leq S_3 \leq 1$).

There are several parameters that frequently occur as alternatives to describing the *SOP* of a light wave by a Stokes vector. These include the degree of polarization (*DOP*), degree of linear polarization (*DOLP*), and degree of circular polarization (*DOCP*). They relate to the Stokes vector as

$$DOP = \frac{\sqrt{S_1^2 + S_2^2 + S_3^2}}{S_0}, \quad DOLP = \frac{\sqrt{S_1^2 + S_2^2}}{S_0}, \quad DOCP = \frac{S_3}{S_0}$$

Polarization is often rendered as an ellipse, indicative of the precession of the electric field in a plane as a light wave passes normally through the plane. The ellipticity e is a measure of the linearity/circularity; an ellipticity of 0 indicates linearly polarized light and an ellipticity of 1 indicates circularly polarized light. The ellipticity of a polarization ellipse relates to the Stokes components as

$$e = \frac{S_3}{1 + \sqrt{S_1^2 + S_2^2}}$$

The azimuth of the major axis of the ellipse α is the angle of the linear-most state, i.e., as the ellipticity approaches zero, the polarization ellipse collapses to a straight line at the angle of the linear state. The angle of the major axis relates to the Stokes vector by

$$\alpha = \frac{1}{2} \tan^{-1} \left(\frac{S_2}{S_1} \right)$$

The notion of ellipticity and handedness of polarization is important. Fig. 1 shows how a quarter-wave retarder can be used to convert linear states into circular states. In both the left- and right-hand cases, a linear state is incident upon a quarter-wave retarder with its fast axis oriented at $+45^\circ$. In each case, the linear state is rendered as two components, one parallel and the other perpendicular to the fast axis of the retarder. Fig. 1 shows precession of the electric field vector as light propagates from the retarder. In Fig. 1a, vertical polarized light is converted to left-hand circular, and in Fig. 1b, horizontal polarized light is converted to right-hand circular.

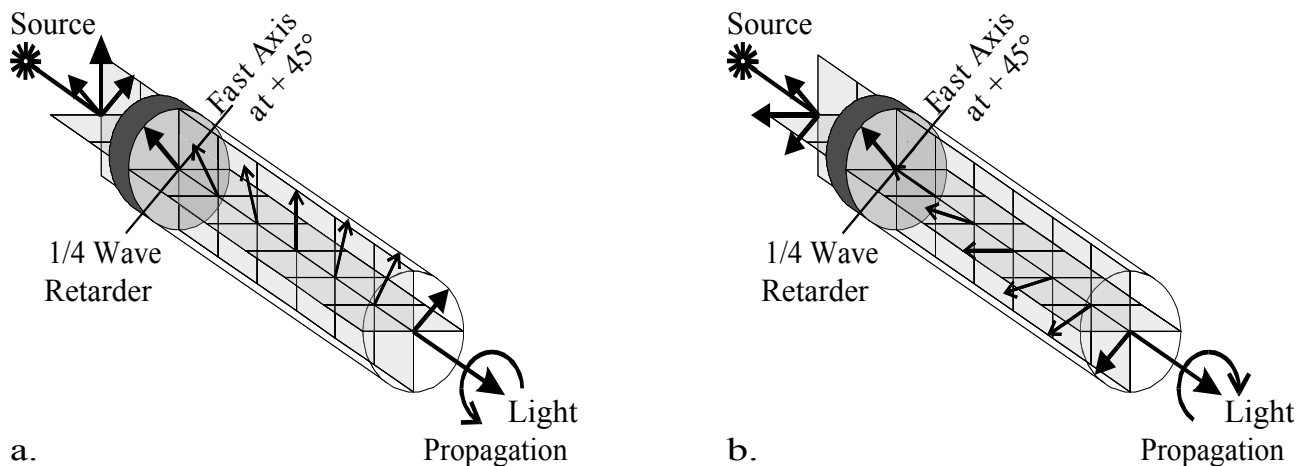


Fig. 1 Left (a) and right (b) circular polarization states, produced by passing linearly polarized light through a quarter-wave retarder with the fast axis at $+45^\circ$

Notice that angles (e.g. the orientation of the retarder's fast axis) and rotational directions (clockwise and counterclockwise) are from the perspective *looking toward the source*.

3. OPTICS & DEVICES USED IN POLARIMETERS

Polarization optics generally affect either the relative magnitudes of perpendicular electric field components or the phase between perpendicular components of a light wave. Here we present a brief overview of polarization optics that are used in polarimetry devices.

Under the category of polarization optics that affect the relative magnitudes of perpendicular components are dichroic polarizers and prism polarizers. Dichroic polarizers use a material that transmits one component and absorbs or reflects the perpendicular component; this is known as diattenuation. Prism polarizers usually redirect orthogonally polarized components in different spatial directions.

Polarization optics that affect the phase between orthogonal components are called retarders or waveplates. The material basis of most retarders is birefringence: one component of a light wave sees a different index of refraction (thus a different optical path length through the material) than the perpendicular component. Commercially available waveplates are specified by the amount of retardance at a particular wavelength, and the fast axis location (the transverse angle at which the index of refraction is minimum).

Reflections at non-normal incidence also produce phase shifts between orthogonal components of the incident light. A component that utilizes this effect is the Fresnel rhomb. Light enters a Fresnel rhomb, undergoes two internal reflections that result in a 90° phase shift, then exits.

Variable retarders are also available; these consist of a material that changes birefringence in the presence of an electric field. Kerr cells, Pockels cells, and liquid crystal cells are all examples of variable retarders. Kerr cells generally use any of several specific organic compounds that change birefringence when a high voltage (~1 kV) is applied across the material. Pockels cells consist of a solid crystal material that undergoes a change in birefringence upon application of high voltage (~1 kV). Liquid crystal variable retarders (LCVR's) are commonly used in low-voltage (~10V) applications. A liquid crystal cell with no voltage applied acts as a retarder, with a retardance proportional to the liquid crystal thickness and LC material birefringence. Application of a voltage causes the liquid crystal molecules to align to the electric field (parallel to the direction of light propagation), thereby reducing (or nearly nullifying with sufficient voltage) the birefringence of the cell.

A LIQUID CRYSTAL POLARIMETER

Here we present a metrology technique by which all four components of the Stokes vector are determined simultaneously. The algorithm presented here is documented in a U.S. Patent (pending) by Davis *et al.*⁶

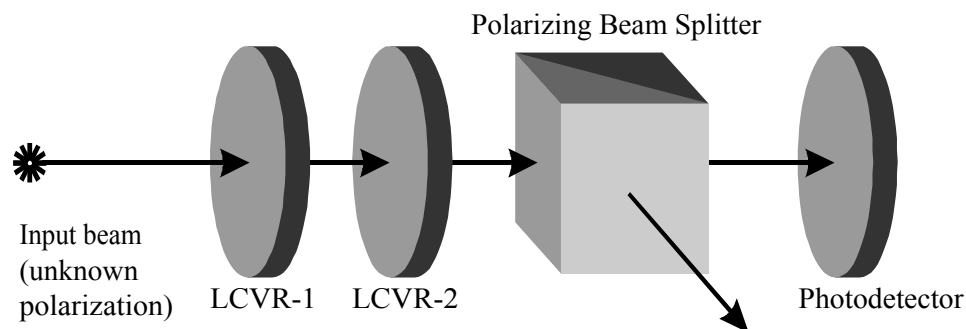


Fig. 2 Optical schematic of a liquid crystal polarimeter

4.1 Optical configuration and modeling

The optical configuration of a liquid crystal polarimeter is shown in Fig. 2. The LCVR's are varied from maximum to minimum retardance, in sequence (i.e., first LCVR-1 is varied, then LCVR-2 is varied). The optics, from incidence of light onto LCVR-1 to detection by the photodetector, are modeled by a time-dependent Mueller matrix

$$M = \begin{bmatrix} a_1(t) & b_1(t) & c_1(t) & d_1(t) \\ a_2(t) & b_2(t) & c_2(t) & d_2(t) \\ a_3(t) & b_3(t) & c_3(t) & d_3(t) \\ a_4(t) & b_4(t) & c_4(t) & d_4(t) \end{bmatrix}$$

A complete interpretation of $\mathbf{M}(t)$ is beyond the scope of the present discussion, and in what follows we will show that only the first row of $\mathbf{M}(t)$ pertains to *SOP* measurements.

4.2. Detection algorithm

When light having a time-invariant *SOP* is incident upon the polarimeter, the *SOP* at the detector is the inner product of the incident Stokes vector and the Mueller matrix describing the optics through which the incident light passed, i.e.,

$$S'(t) = \begin{bmatrix} S'_0(t) \\ S'_1(t) \\ S'_2(t) \\ S'_3(t) \end{bmatrix} = \begin{bmatrix} a_1(t) & b_1(t) & c_1(t) & d_1(t) \\ a_2(t) & b_2(t) & c_2(t) & d_2(t) \\ a_3(t) & b_3(t) & c_3(t) & d_3(t) \\ a_4(t) & b_4(t) & c_4(t) & d_4(t) \end{bmatrix} \bullet \begin{bmatrix} S_0 \\ S_1 \\ S_2 \\ S_3 \end{bmatrix}$$

where $S'(t)$ is a time-varying Stokes vector that models the *SOP* of light that has passed through the polarimeter optics. Since the photodetector is capable of measuring intensities only, the signal returned from the photodetector is $S'_0(t)$ which relates to the incident Stokes vector by

$$S'_0(t) = S_0 a_1(t) + S_1 b_1(t) + S_2 c_1(t) + S_3 d_1(t)$$

Therefore, if the first row of $\mathbf{M}(t)$ is known at four points in time and $S'_0(t)$ is measured at the same four points in time a system of four equations follows. The solution to this system of equations are the components of \mathbf{S} . In practice, $a_1(t)$, $b_1(t)$, $c_1(t)$, and $d_1(t)$ are sampled as the two LCVR's are varied and \mathbf{S} is calculated by a least-squares fit to improve statistical accuracy.

5. Calibration Procedure

Calibration is a sequence of measurements where six known polarization states \mathbf{S} are applied to determine $a_1(t)$, $b_1(t)$, $c_1(t)$, and $d_1(t)$. The first two applied polarization states are horizontal and vertical. The Stokes vectors that indicate horizontal (S_H) and vertical (S_V) polarization are

$$S_H = \begin{bmatrix} \hat{e} & 1 & \hat{u} \\ \hat{e} & 1 & \hat{u} \\ \hat{e} & 0 & \hat{u} \\ \hat{e} & 0 & \hat{u} \end{bmatrix} \quad S_V = \begin{bmatrix} \hat{e} & 1 & \hat{u} \\ \hat{e} & -1 & \hat{u} \\ \hat{e} & 0 & \hat{u} \\ \hat{e} & 0 & \hat{u} \end{bmatrix}$$

The detected time-varying signals $S'_{0}(t)$ resulting from horizontal and vertical linearly polarized light are

$$S_{\mathcal{G}_H}(t) = a_1(t) + b_1(t) \quad \text{and} \quad S_{\mathcal{G}_V}(t) = a_1(t) - b_1(t)$$

respectively.

From these two measurements, $a_1(t)$ and $b_1(t)$ are determined by

$$\begin{aligned} S_{\mathcal{G}_H}(t) &= a_1(t) + b_1(t) \\ S_{\mathcal{G}_V}(t) &= a_1(t) - b_1(t) \end{aligned} \quad \begin{aligned} a_1(t) &= \frac{1}{2}(S_{\mathcal{G}_H}(t) + S_{\mathcal{G}_V}(t)) \\ b_1(t) &= \frac{1}{2}(S_{\mathcal{G}_H}(t) - S_{\mathcal{G}_V}(t)) \end{aligned}$$

In a similar manner, the Stokes vectors that indicate $\pm 45^\circ$ linear and right- and left-circular polarization states respectively are

$$\begin{aligned} \mathbf{S}_{+45} &= \begin{pmatrix} \hat{e}_1 \cdot \hat{u} \\ \hat{e}_0 \cdot \hat{u} \\ \hat{e}_1 \cdot \hat{v} \\ \hat{e}_0 \cdot \hat{v} \end{pmatrix} & \mathbf{S}_{-45} &= \begin{pmatrix} \hat{e}_1 \cdot \hat{u} \\ \hat{e}_0 \cdot \hat{u} \\ \hat{e}_- \cdot \hat{v} \\ \hat{e}_0 \cdot \hat{v} \end{pmatrix} & \mathbf{S}_R &= \begin{pmatrix} \hat{e}_1 \cdot \hat{u} \\ \hat{e}_0 \cdot \hat{u} \\ \hat{e}_0 \cdot \hat{v} \\ \hat{e}_1 \cdot \hat{v} \end{pmatrix} & \mathbf{S}_L &= \begin{pmatrix} \hat{e}_1 \cdot \hat{u} \\ \hat{e}_0 \cdot \hat{u} \\ \hat{e}_0 \cdot \hat{v} \\ \hat{e}_- \cdot \hat{v} \end{pmatrix} \end{aligned}$$

The two time-varying signals measured when $\pm 45^\circ$ linear states are incident upon the detector give $c_1(t)$ by

$$\begin{aligned} S_{\mathcal{G}_{+45}}(t) &= a_1(t) + c_1(t) \\ S_{\mathcal{G}_{-45}}(t) &= a_1(t) - c_1(t) \end{aligned} \quad c_1(t) = \frac{1}{2}(S_{\mathcal{G}_{+45}}(t) - S_{\mathcal{G}_{-45}}(t))$$

The two signals measured when right and left circular states are incident upon the detector give $d_1(t)$ by

$$\begin{aligned} S_{\mathcal{G}_R}(t) &= a_1(t) + d_1(t) \\ S_{\mathcal{G}_L}(t) &= a_1(t) - d_1(t) \end{aligned} \quad d_1(t) = \frac{1}{2}(S_{\mathcal{G}_R}(t) - S_{\mathcal{G}_L}(t))$$

Note that this six-measurement sequence lets one redundantly calculate $a_1(t)$. Just as $a_1(t)$ is proportional to the sum of the first two measurements, it is similarly proportional to the sum of the two signals detected when the $\pm 45^\circ$ linear states are applied, and it is proportional to the sum of the two signals detected when the right and left circular states are applied. Therefore, a simplified four-step calibration proceeds with the first two measurements (using horizontal and vertical incident light) as described to determine $a_1(t)$ and $b_1(t)$. Next, either the $+45^\circ$ or -45° measurement is performed and $c_1(t)$ is calculated as the difference between the measured signal and $a_1(t)$. Finally, $d_1(t)$ can be determined as the difference between $a_1(t)$ and one measurement when either right or left circular light is applied.

6. UNCERTAINTIES

6.1 Precision and accuracy of Stokes parameters

A formal derivation of the estimated uncertainty in the Stokes parameters measured by a liquid crystal polarimeter will be the topic of a forthcoming paper. For now we present empirical uncertainties for a LCPM-3000 liquid crystal polarimeter from Meadowlark Optics, Inc. Nineteen states of polarization

were made incident (sequentially) on the polarimeter, and fifty measurements were made of each SOP. Each measurement takes ~1 second. The intensity incident upon the entrance aperture of the polarimeter was ~2mW; this level of irradiance is sufficient for good dynamic range without saturating the detectors. The uncertainty in each of the Stokes parameters was calculated as the standard deviation of each set of fifty measurements. Table 1 shows the average and maximum of the nineteen uncertainties.

Table1: Stokes uncertainties

Stokes parameter	Mean uncertainty	Maximum uncertainty
S ₀	5.21×10 ⁻⁴	2.00×10 ⁻³
S ₁	5.95×10 ⁻⁴	2.00×10 ⁻³
S ₂	4.32×10 ⁻⁴	1.00×10 ⁻³
S ₃	1.65×10 ⁻³	5.00×10 ⁻³

6.2 Error propagation from the measured Stokes vector

Several polarization parameters are calculated from the Stokes vector components. Uncertainties in the measured Stokes components can be propagated to obtain uncertainties of calculated parameters. The error propagation methods used here are adapted from standard techniques of Bevington and Robinson.⁷

6.2.1 Uncertainty in the DOP

The degree of polarization is calculated from the Stokes parameters as shown in in eq. (2). The uncertainty in the degree of polarization due to uncertainties in each element of the Stokes vector is

$$s_{DOP} = \sqrt{s_0^2 \left(\frac{\partial DOP}{\partial S_0}\right)^2 + s_1^2 \left(\frac{\partial DOP}{\partial S_1}\right)^2 + s_2^2 \left(\frac{\partial DOP}{\partial S_2}\right)^2 + s_3^2 \left(\frac{\partial DOP}{\partial S_3}\right)^2}$$

Assuming equal uncertainties in the measured Stokes parameters ($s_i = s$ for $i = 0,1,2,3$) and evaluating the partial derivative of the DOP [eq. (2)] with respect to each of the Stokes parameters and

$$s_{DOP} = \sqrt{s^2 \frac{S_1^2 + S_2^2 + S_3^2}{S_0^4} + s^2 \frac{S_1^2}{S_0^2 (S_1^2 + S_2^2 + S_3^2)} + s^2 \frac{S_2^2}{S_0^2 (S_1^2 + S_2^2 + S_3^2)} + s^2 \frac{S_3^2}{S_0^2 (S_1^2 + S_2^2 + S_3^2)}}$$

substituting gives

which reduces to

$$s_{DOP} = s \frac{\sqrt{S_0^2 + S_1^2 + S_2^2 + S_3^2}}{S_0^2}$$

Since S₀ and the DOP are both ~1 (recall that the $DOP \propto \sqrt{S_1^2 + S_2^2 + S_3^2}$), eq. (2) is nominally 1.4□.

6.2.2 Uncertainty in the DOLP

The DOLP expression in eq. (2) is mathematically similar to that of the DOP in eq. (2) without the S_3 term. The uncertainty in the degree of linear polarization due to Stokes measurement uncertainties s occurring in each of the Stokes parameters is

$$s_{DOLP} = \sqrt{s_{0e}^2 \frac{\partial DOLP}{\partial S_0}^2 + s_{1e}^2 \frac{\partial DOLP}{\partial S_1}^2 + s_{2e}^2 \frac{\partial DOLP}{\partial S_2}^2 + s_{3e}^2 \frac{\partial DOLP}{\partial S_3}^2}$$

Substituting the partial derivatives of the DOLP with respect to each of the Stokes parameters and noting that the Stokes parameter uncertainties all equal s gives

$$s_{DOLP} = \sqrt{s^2 \frac{S_1^2 + S_2^2}{S_0^4} + s^2 \frac{S_1^2}{S_0^2(S_1^2 + S_2^2)} + s^2 \frac{S_2^2}{S_0^2(S_1^2 + S_2^2)}}$$

which reduces to

$$s_{DOLP} = s \frac{\sqrt{S_0^2 + S_1^2 + S_2^2}}{S_0^2}$$

Again we will assume that $S_0 \sim 1$. As the SOP approaches a circular state, S_1 and S_2 both approach zero, and $\square_{DOLP} \sim \square$. As the SOP approaches a linear state, \square_{DOLP} approaches 1, and \square_{DOLP} approaches $1.4\square$.

6.2.3 Uncertainty in the DOCP

The degree of circular polarization is the ratio S_3/S_0 as expressed in eq. (2). Uncertainty in the DOCP due to measurement errors in S_0 and S_3 is

$$s_{DOCP} = \sqrt{s_{0e}^2 \frac{\partial DOCP}{\partial S_0}^2 + s_{3e}^2 \frac{\partial DOCP}{\partial S_3}^2}$$

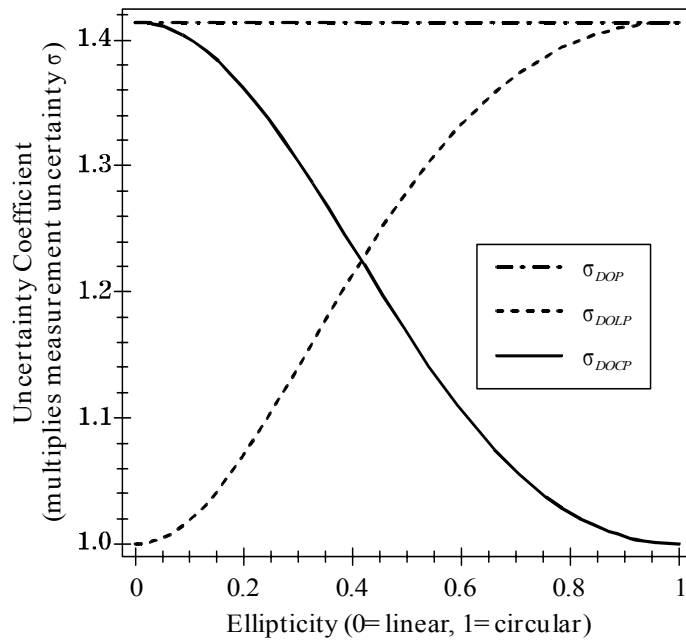
Note that the uncertainty in \square_{DOCP} is independent of S_1 and S_2 . Substituting expressions for the partial derivatives of the DOCP with respect to S_0 and S_3 gives

$$s_{DOCP} = \sqrt{s^2 \frac{S_3^2}{S_0^4} + s^2 \frac{1}{S_0^2}} = s \frac{\sqrt{S_0^2 + S_3^2}}{S_0^2}$$

Again we assume that $S_0 \sim 1$. As the DOCP varies from 0 (purely linear state, $S_3=0$) to 1 (purely circular state, $S_3=1$), the uncertainty in the DOCP varies from \square to $1.41\square$.

6.2.4 Graphical comparison of \square_{DOP} , \square_{DOLP} , and \square_{DOCP}

It was mentioned in the previous three derivations how \square_{DOP} , \square_{DOLP} , and \square_{DOCP} varied as light changes from a linear state to a circular state. Here we plot these uncertainties as the SOP changes uniformly from linear to circular.



This plot shows that the uncertainty in the calculated DOP is insensitive to ellipticity. Regarding uncertainty in the calculated degree of linear polarization, this plot shows that σ_{DOLP} is minimum when the SOP is linear and σ_{DOLP} increases as the SOP becomes more circular. Regarding uncertainty in the calculated degree of circular polarization, this plot shows that σ_{DOCP} is maximum when the SOP is linear and σ_{DOCP} decreases as the SOP becomes more circular.

6.2.5 Uncertainty in σ .

The ellipticity is calculated from S_1 , S_2 , and S_3 as shown in eq. (3). The ellipticity uncertainty σ_e due to uncertainties σ_1 , σ_2 and σ_3 is

$$\sigma_e = \sqrt{s_1^2 \frac{\partial \sigma}{\partial S_1}^2 + s_2^2 \frac{\partial \sigma}{\partial S_2}^2 + s_3^2 \frac{\partial \sigma}{\partial S_3}^2}$$

Substituting the partial derivatives of σ with respect to σ_1 , σ_2 , and σ_3 gives

$$\sigma_e = \sqrt{s_1^2 \frac{S_1^2 S_3^2}{(S_1^2 + S_2^2)(1 + \sqrt{S_1^2 + S_2^2})^4} + s_2^2 \frac{S_2^2 S_3^2}{(S_1^2 + S_2^2)(1 + \sqrt{S_1^2 + S_2^2})^4} + s_3^2 \frac{1}{(1 + \sqrt{S_1^2 + S_2^2})^2}}$$

Assuming $\sigma_1 = \sigma_2 = \sigma_3 = \sigma$ and reducing, we get

$$\sigma_e = \sigma \sqrt{\frac{S_3^2}{(1 + \sqrt{S_1^2 + S_2^2})^4} + \frac{1}{(1 + \sqrt{S_1^2 + S_2^2})^2}}$$

This result is plotted as the SOP was varied from linear to circular.

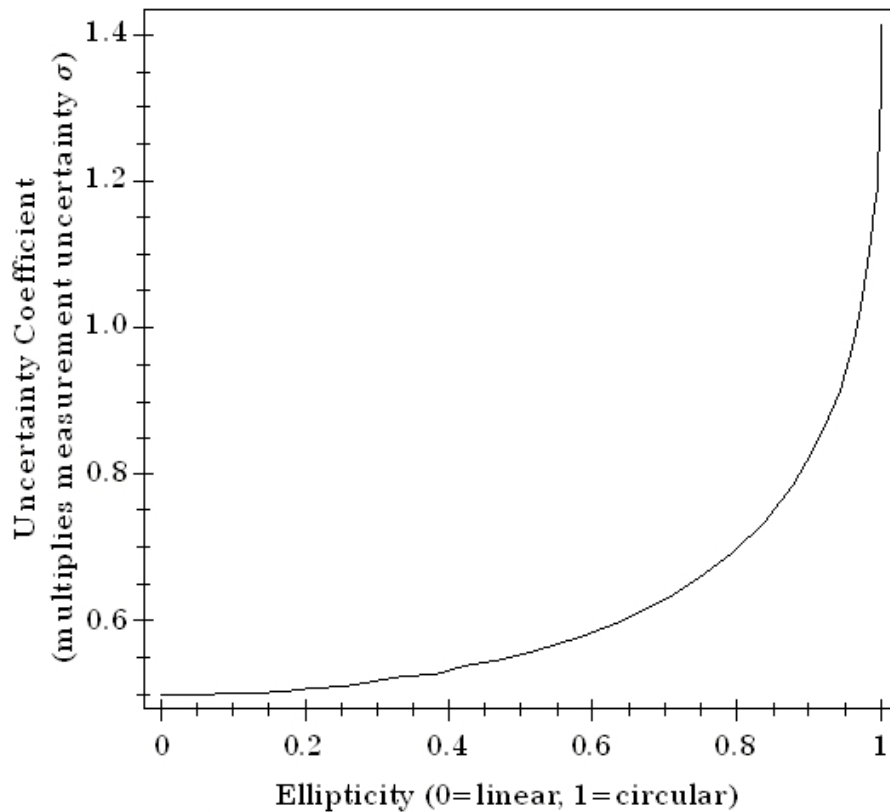


Fig. 4 Ellipticity uncertainty as ellipticity was varied.

Assuming $S_0 \sim 1$ and fully polarized light, the ellipticity uncertainty σ_e assumes a minimum value of 0.5σ when the SOP is linear (i.e., $S_3=0$) and a maximum value of 1.4σ when the SOP is circular.

6.2.6 Uncertainty in α .

The azimuth of the polarization ellipse is calculated in eq. (4) from S_1 and S_2 . The uncertainty in the azimuth due to uncertainties σ_1 and σ_2 is

$$s_a = \sqrt{s_1^2 \left(\frac{\partial \alpha}{\partial S_1} \right)^2 + s_2^2 \left(\frac{\partial \alpha}{\partial S_2} \right)^2}$$

Substituting the partial derivatives of α with respect to σ_1 and σ_2 gives

$$\alpha = \arctan \left(\frac{E_V}{E_H} \right) = \arctan \left(\frac{\sqrt{I_V}}{\sqrt{I_H}} \right)$$

Assuming $\sigma_1 = \sigma_2 = \sigma$ and reducing gives

$$s_a = s \frac{1}{2} \sqrt{\frac{1}{S_1^2 + S_2^2}}$$

This result is plotted versus ellipticity, assuming fully polarized light.

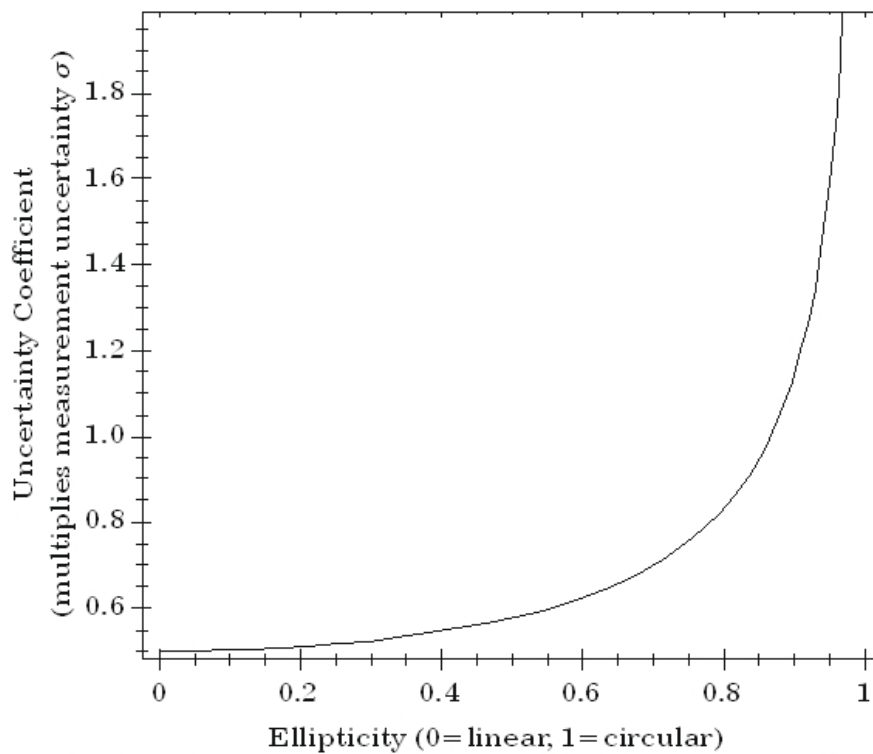
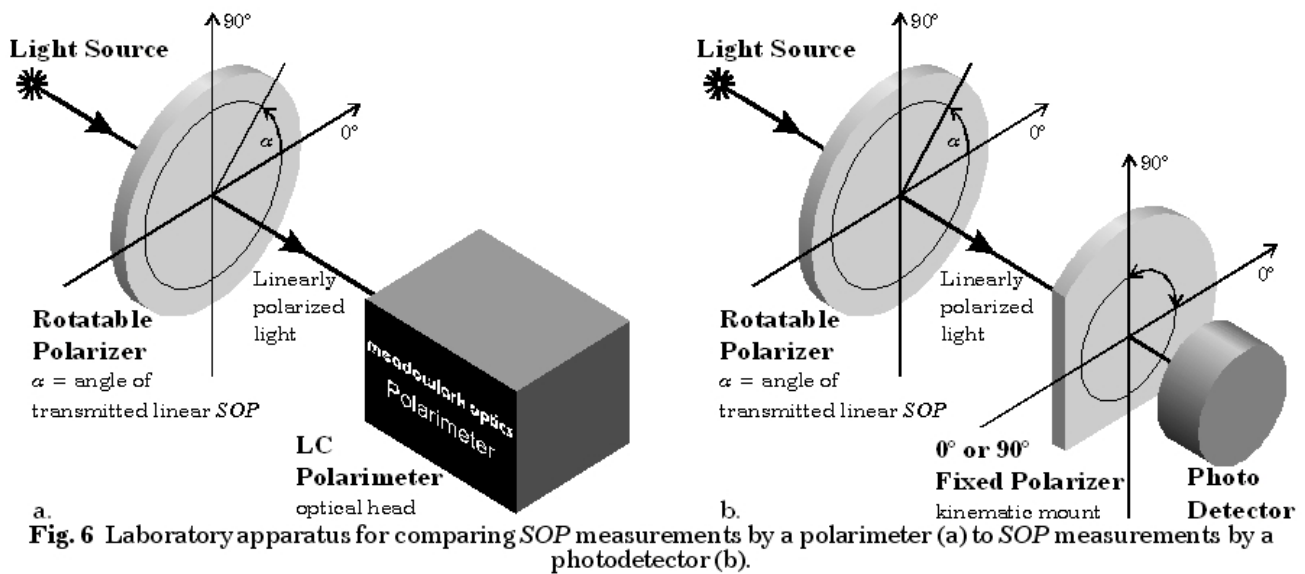


Fig. 5 Azimuth uncertainty as ellipticity was varied.

The uncertainty in a due to uncertainty in the measured Stokes parameters is $0.5\sqrt{a}$ for linear states, and grows without bound as the state becomes circular. This is due to the ambiguity of the ellipse's angle in a purely circular state.

7. LABORATORY TESTING

An experiment was conducted in which SOP measurements by a polarimeter and by a photodetector with a polarizer in front are compared. The apparatus for these experiments is shown in Fig. 6.



The experiment proceeded as follows: unpolarized, monochromatic ($\lambda=633\text{ nm}$) light was directed through a rotatable polarizer to produce a linear state at a selectable angle α . A liquid crystal polarimeter (LCPM-3000 by Meadowlark Optics, Inc.) was used to measure the SOP of the polarized beam as shown in Fig. 6a. A kinematic mount was configured so that a photodetector (ThorLabs PDA55, readout on a Fluke 77III multimeter) could be placed in or out of the beam, ahead of the polarimeter head. A second specialized kinematic mount (ESGS-633 by Meadowlark Optics, Inc.) was used so that a polarizer could be removed or placed to allow either vertical or horizontal light to arrive at the photodetector, as shown in Fig. 6b. In this way, the vertical, horizontal, and combined intensity components of the linear SOP (I_H , I_V , and I_C , respectively) were measured with the photodetector. The angle of the linear polarization state α was calculated by eq. (4) using Stokes vector components acquired with the polarimeter. The angle α was also calculated from photodetector measurements of I_H and I_V by

$$\alpha = \arctan\left(\frac{E_V}{E_H}\right) = \arctan\left(\frac{\sqrt{I_V}}{\sqrt{I_H}}\right)$$

where E_V and E_H are the vertical and horizontal components of electric field vector, respectively. Recall that the angle of the electric field vector is the angle of polarization.

The liquid crystal polarimeter was calibrated and a background reading was taken according to the manufacturer's instructions. A background measurement was acquired with the photodetector and subtracted from each reading.

The angle α of the rotatable polarizer was incremented from $-\pi/2$ to $\pi/2$ radians in increments of $\sim\pi/18$. The linear SOP was measured as Stokes components with the polarimeter, and the vertical and horizontal, and combined intensity components of the linear SOP were measured with the photodetector at each increment. Angles calculated from both techniques are plotted in Fig. 7, and the discrepancies between polarimeter measurements and corresponding photodetector measurements are plotted in Fig. 8.

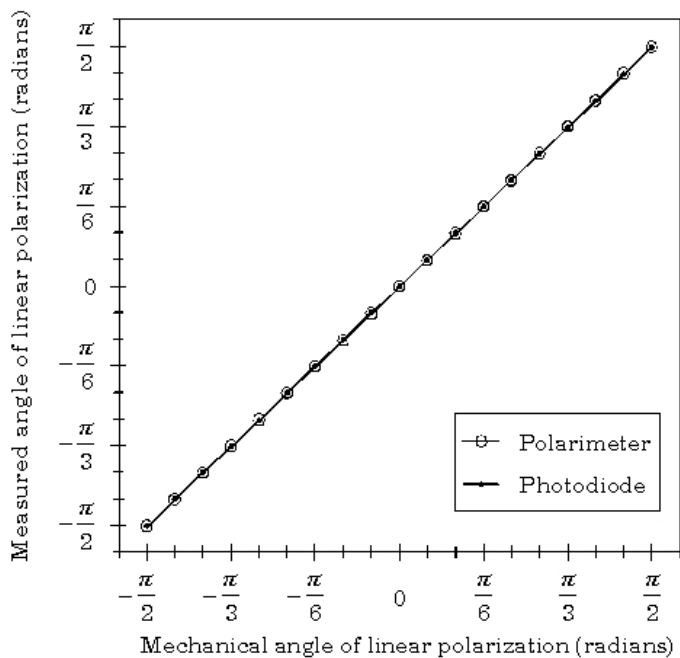


Fig. 7 Empirical polarization angles.

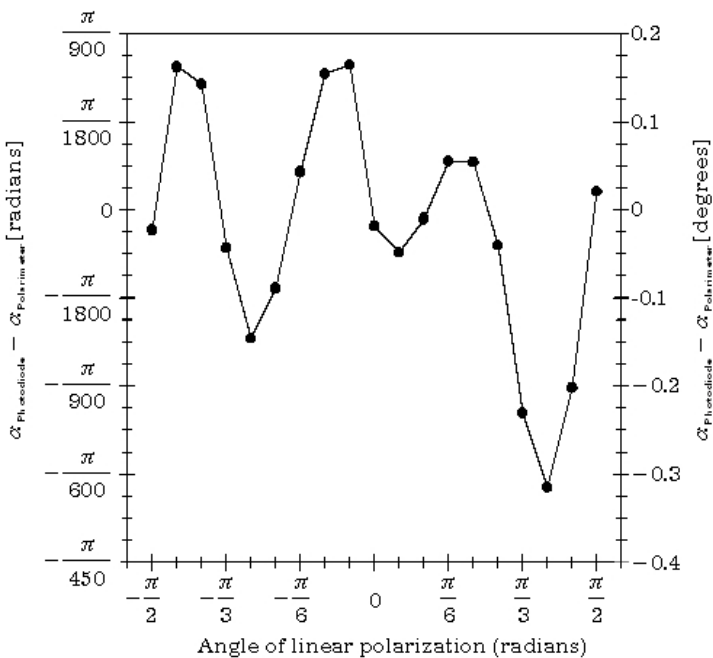


Fig. 8 Polarization angle differences

Note that the nominal difference between polarization angle values calculated from polarimeter measurements and angle values calculated from photodetector measurements is less than 5×10^{-3} radians. The observed discrepancy is well within the predicted uncertainty.

8. CONCLUSIONS

We have modeled the methodology and tested the accuracy of a liquid crystal polarimeter from Meadowlark Optics, Inc. The algorithm by which this device conducts polarimetry measurements employs a sequential sweep of two liquid crystal variable retarders. The effect of sweeping two retarders on the polarization state of incident light is defined in a calibration procedure using known input states; the device then uses this definition to resolve the unknown SOP of incident light.

A detailed treatment of the uncertainty in each of the four Stokes parameters is forthcoming. In the meantime, the repeatability of SOP measurements provided an estimated measurement uncertainty of $<0.2\%$ in each component of the Stokes vector. A comparison of polarization angle measurements made with the liquid crystal polarimeter to measurements made using a photodetector and polarizer agreed within $\pm 0.3^\circ$.

REFERENCES

1. T. Baur, "Optical Polarimeters for Solar Research," *Opt. Eng.* 20, 2 (1981).
2. E. Hecht, A. Zajac, *Optics*, (Addison-Wesley, Menlo Park, California, 1979).
3. M. Born, E. Wolf, *Principles of Optics*, (Pergamon Press, Oxford, 1980).

4. W. A. Shurcliff, Polarized Light: Production and Use, (Harvard University Press, Cambridge, Mass., 1966).

5. D. S. Kliger, J.W. Lewis, C. E. Randall, Polarized Light in Optics and Spectroscopy, (Academic Press, San Diego, California, 1990).

6. S. R. Davis, R. J. Uberna, R. A. Herke. Retardance Sweep Polarimeter and Method. U.S. Patent Pending, Application No. 10/224,041 (2004).

7. P. R. Bevington, D. K. Robinson. Data Reduction and Error Analysis for the Physical Sciences, 2nd Ed., (WCB/McGraw-Hill, Boston, Massachusetts, 1992).